



# STREAMS

Smart Technologies for eneRgy Efficient Active  
cooling in Advanced Microelectronic Systems



H2020-ICT-2015-688564

## **STREAMS**

### **Smart Technologies for eneRgy Efficient Active cooling in advanced Microelectronic Systems**

Start date of the project: 01/01/2016  
Duration: 42 months

#### **D6.1**

### **Technical report on the predicted thermal map, comparison with measurements**

<b>WP</b>	6	Performances assessment in future applications
<b>Task</b>	6.1	Complete thermal simulation model at interposer level

<b>Dissemination Level<sup>1</sup></b>	PU	<b>Due Delivery Date</b>	M42
<b>Nature<sup>2</sup></b>	R	<b>Actual Delivery Date</b>	26/07/2019

<b>Lead beneficiary</b>	UdL
<b>Contributing beneficiaries</b>	UdL, ST

<b>Author</b>	<b>Proofreader</b>
J. Barrau	P. Coudrain

<sup>1</sup> Dissemination level: **PU** = Public, **PP** = Restricted to other programme participants (including the Commission services), **RE** = Restricted to a group specified by the consortium (including the JU), **CO** = Confidential, only for members of the consortium (including the Commission services).

<sup>2</sup> Nature of the deliverable: **R** = Report, **D** = Demonstrator, **O** = Other.

Document version	Date	Author	Comments <sup>3</sup>
v1	24/07/2019	J. Barrau (UdL)	Creation
v2	25/07/2019	P. Coudrain (ST)	Modification
v3	26/07/2019	J. Barrau (UdL)	Final version for evaluation

---

<sup>3</sup> Creation, modification, final version for evaluation, revised version following evaluation, final.

## Content

1. INTRODUCTION .....	4
2. METHODOLOGY.....	4
3. CFD model .....	5
3.1. Description .....	5
3.2. Results 3x3 cell matrix.....	6
3.3. Array study .....	7
3.4. 3x3 flipped cell matrix .....	8
3.5. Conclusion and future works.....	9
4. Numerical tool (Matlab).....	10
4.1. Hydraulic and thermal modeling.....	10
4.2. Boundary conditions .....	13
4.3. Main results.....	14
4.4. Conclusion and future works.....	18
5. IC-THERM.....	19
5.1. Computational model.....	19
5.2. Discretization of the Heat Equation .....	20
5.3. Solvers .....	22
5.4. Usage of the initial simulator .....	22
5.5. Modifications proposal of the algorithm to adapt to the STREAMS case.....	23
5.6. Implementation.....	24
5.7. Conclusion and future works.....	24
6. CONCLUSIONS AND FUTURE WORK.....	25

## 1. INTRODUCTION

After validating the solutions implemented along the STREAMS project, this Deliverable aims at developing a numerical model that incorporates the chips with the interposer and its smart features. Parametric studies will allow assessing the impact of several parameters on the performance of the STREAMS solutions.

## 2. METHODOLOGY

The objectives defined in Task 6.1 required the development of new tools that did not exist at the beginning of this project. The task to be developed is even more challenging when considering the smart behavior of the STREAMS cooling solution.

Consequently, it has been decided to work on 3 different tools in order to investigate their performance and limitations:

- 1- A CFD model, taking into account the self-adaptive behavior of the STREAMS solution and the spreading effects has been implemented.
- 2- A numerical tool, based on Matlab, allows predicting the flow rate distribution through the array of microfluidic cells and its impact on the chip temperature distribution.
- 3- A sub-millimetric model (called IC-THERM), oriented to microelectronics applications, allows the assessment of temperature distributions in 3D architectures.

Each of these models is described in the following chapters together with the main results obtained.

For each of them, the cooling solution consists in a matrix of 6\*10 microfluidic cells (Figure 1) which have the geometry identified in WP2 as MC6T. A self-adaptive valve, located at the outlet of each microfluidic cell, tailors the local flow rate.

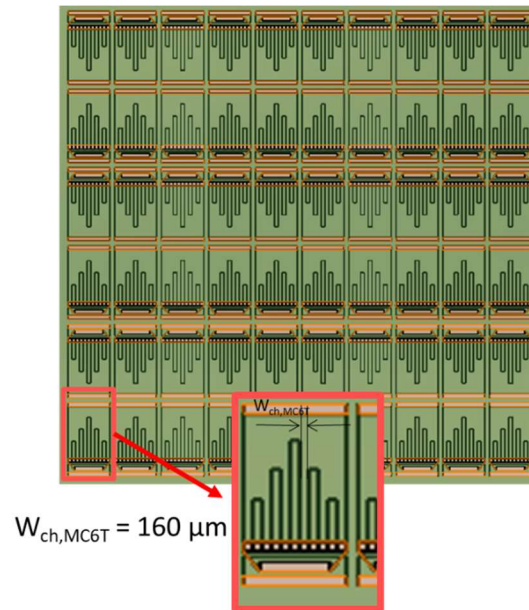


Figure 1 Matrix of 6\*10 microfluidic cells with detail of MC6T cell geometry

### 3. CFD model

#### 3.1. Description

To assess the spreading between the cells, a 3 by 3 cell matrix is taken into consideration shown in (Figure 2). To simplify the study, the heat loads are uniform on the base of each cell. In this matrix, all the perimeter cells are set to 20 W/cm<sup>2</sup> and in the center is placed the hotspot to 20, 60, 80 or 300 W/cm<sup>2</sup>.

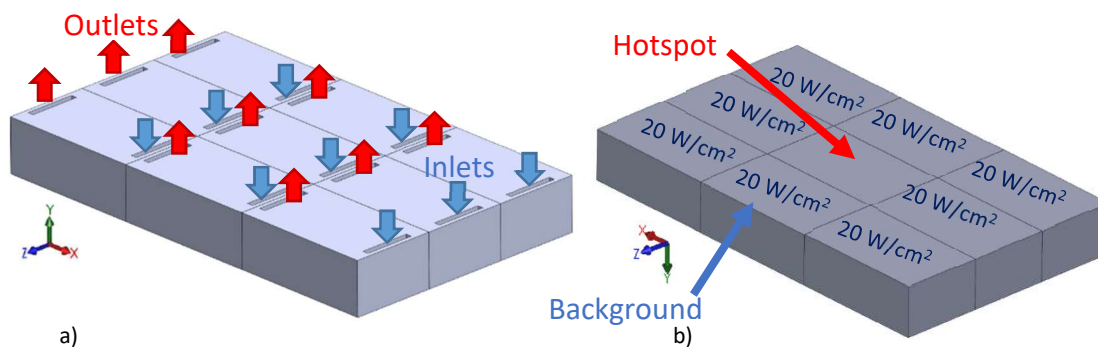


Figure 2. a) Matrix of microfluidic cells b) Power density distribution with the hotspot at the center

The flow rate of each cell is the flow needed to maintain the base maximum temperature of an isolated cell below 85°C with an inlet flow temperature of 50°C. The isolated cell evaluation with different heat fluxes and the temperature limitation on the base is represented in Table 1.

The CFD model has been implemented through COMSOL-Multiphysics®.

*Table 1. Evaluation of one cell isolated*

<b>q'' (W/cm<sup>2</sup>)</b>	<b>P<sub>in</sub> (W)</b>	<b>Q<sub>cell</sub> (mL/min)</b>	<b>ΔP (Pa)</b>	<b>T<sub>chip,average</sub> (°C)</b>	<b>ΔT<sub>chip</sub> (°C)</b>	<b>R (cm<sup>2</sup>°C/W)</b>	<b>P<sub>pump</sub> (W)</b>	<b>COP (-)</b>
<b>300</b>	9.51	32.43	46525	80.0	10.3	0.100	1.3·10 <sup>-2</sup>	7.6·10 <sup>2</sup>
<b>80</b>	2.53	2.89	552	81.7	7.7	0.396	1.3·10 <sup>-5</sup>	1.9·10 <sup>5</sup>
<b>60</b>	1.90	1.99	305	81.7	7.6	0.528	5.1·10 <sup>-6</sup>	3.8·10 <sup>5</sup>
<b>20</b>	0.63	0.56	52	82.7	5.4	1.634	2.5·10 <sup>-7</sup>	2.6·10 <sup>6</sup>

### 3.2. Results 3x3 cell matrix

The 3x3 cell matrix is evaluated with the four heat fluxes scenarios. A different behaviour between the X and Y axes can be seen in the representation of the microfluidic cells base temperature (Figure 3). This effect is the result of the cell disposition, the cell inlet is next to the outlet of the previous one, so in this zone there is a significant heat conduction from the outlet to the inlet flow.

In the case with 20 W/cm<sup>2</sup>, there is no heat flux between cells in the X axe, the Y axe thermal conduction effect represents, depending in each cell position, a cell power absorption reduction of 11% to an increase of 15% of power absorption.

In the 60 and 80 W/cm<sup>2</sup> hotspots cases the difference of heat absorption from each cell is lower than 6% in comparison with the 20 W/cm<sup>2</sup> case. This difference is due to an increase of heat transfer in the X axis. However, the X axis heat transfer has a negligible effect in comparison with the Y axis one (Figure 3).

On the other hand, the microfluidic cell matrix with the 300 W/cm<sup>2</sup> hotspot presents lateral conduction. This is due to the high flow rate that cools down all the lateral walls and absorbs heat from the lateral cells. The average power absorption of the 3x3 matrix background cells with 300 W/cm<sup>2</sup> in the hotspot are between 68 and 71% of the power delivered, with the other heat fluxes conditions the average absorption is between 96 and 101%.

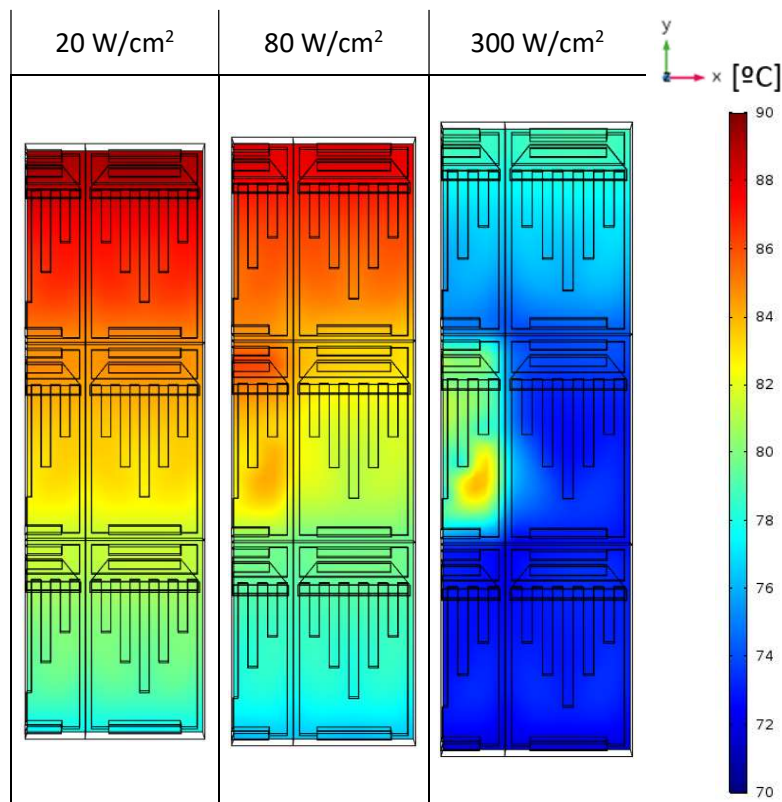


Figure 3 .Microfluidic cell 3x3 matrix thermal map with symmetry ( $z=0$ )

The implications of the Y axis spreading effect is the increase of temperature along the Y axis (Figure 3). The effect is slightly mitigated when the central cell is submitted to  $300 \text{ W/cm}^2$  because the lateral walls of the central cell are cooling the adjacent cells.

### 3.3. Array study

One of the desired characteristics of the microfluidic system is to uncouple the cell working point from the cell position in the matrix. Cells behaviour varies because of the Y-axis spreading, for this are analyzed two cell arrays of 6 microfluidic cells, one with the actual configuration and another with one of every 2 cells flipped in order to have the inlet wall of one cell in contact with the inlet wall of another cell. The cells were submitted to the same boundary conditions as the 3x3 microfluidic cell matrix but with all the cells at  $20 \text{ W/cm}^2$  because most of the cells will be frequently at the background heat flux where the Y-axis spreading is more noticed.

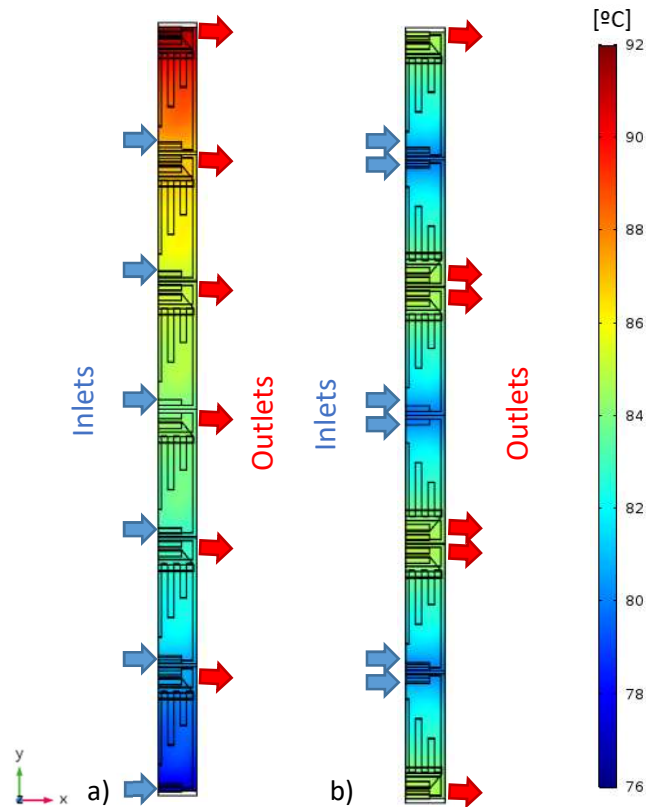


Figure 4. Microfluidic array 1x6 thermal map ( $BT=125\mu\text{m}$ ) a) initial configuration b) flip configuration

With the flip configuration the uniformity of temperature is increased from  $14.3^\circ\text{C}$  for the initial configuration to  $5.5^\circ\text{C}$  for the flip configuration with the same boundary conditions and flow rate. The flip configuration uniformity of temperature matches with the cell isolated ( $5.4^\circ\text{C}$ , Table 1) and the maximum heat transfer between cells were  $0.6\text{W}$  with the initial configuration and  $6 \cdot 10^{-5}\text{W}$  with the flip configuration. With these results, it can be concluded that the Y-axis conduction is avoided with the flip configuration.

#### 3.4. 3x3 flipped cell matrix

As the flipped cell configuration avoid the Y-axis spreading () is analyzed a 3x3 flipped cell matrix in order to determinate the matrix behavior in X and Y directions with different heat fluxes. The boundary conditions are the same as the exposed in the 3x3 cell matrix.

This change of configuration also implies a change in the distributor in which each ramification connected to the microfluidic cells are wider in order to match the two lines of cell with the inlet or outlet in contact.



The temperature uniformity of the 3x3 flipped cell matrix varies depending on the difference of heat flux between the microfluidic cells (Figure 5). This effect is due to the increase of coolant in the central cell that cools down the walls of the adjacent cells also observed with the initial configuration but now is the principal spreading effect because the Y-axis spreading is avoided in this configuration.

The initial 3x3 configuration with all the heat flux configurations had a temperature gradient along the Y axis, so the chip temperature was dependent on the chip surface zone (Figure 3). With the applied changes, the temperature is independent to the chip surface zone (Figure 5). The cell temperature only varies if some adjacent cell is submitted to high heat flux, this effect was also observed in the previous configuration but with the elimination of the Y-axis spreading now is the predominating spreading effect.

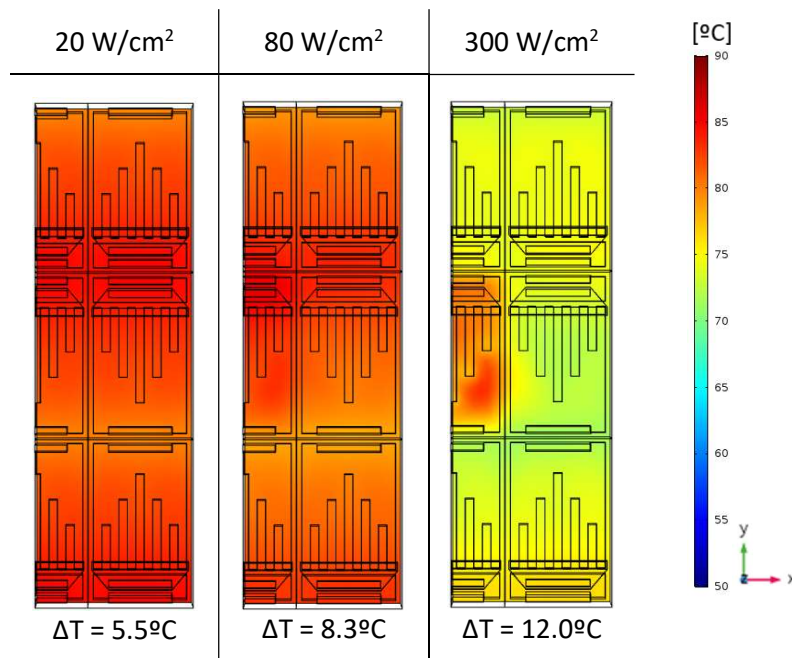


Figure 5. Flipped cell matrix 3x3 thermal maps (BT=125μm)

For this temperature uniformity improvement with the flip configuration the fabricated devices are fabricated with this configuration.

### 3.5. Conclusion and future works

This CFD model has been, at a first stage, a tool for the distributor and cell arrangement definition. At a second stage, we aim at using it for assessment of the performance of the STREAMS solution in future applications.

At this stage, the experimental validation of the model is ongoing. The main limitations of this tool with respect to the objectives of Task 6.1 are related to the high requirements of computational resources.

## 4. Numerical tool (Matlab)

### 4.1. Hydraulic and thermal modeling

The hydraulic circuit under a cell is composed by the cellular tube (or channel) and the thermal valve arranged in series (Fig. 1). The flow of fluid  $Q$  is driven by the difference in pressure between the input section and the output section. The pressure drops, both in the cellular tube and in the valve, are given by an expression of the type

$$\Delta P_i = K_i Q^{n_i} \quad (1)$$

where  $K_i$  and  $n_i$  are constant in the cell tube but in the valve they depend on their working temperature ( $T_{valv}$ ). Then the pressure drop between the input and output sections is:

$$\Delta P = \Delta P_{tc} + \Delta P_{valv} = K_{tc} Q^{n_{tc}} + K_v(T_{valv}) Q^{n_{tc}(T_{valv})}. \quad (2)$$

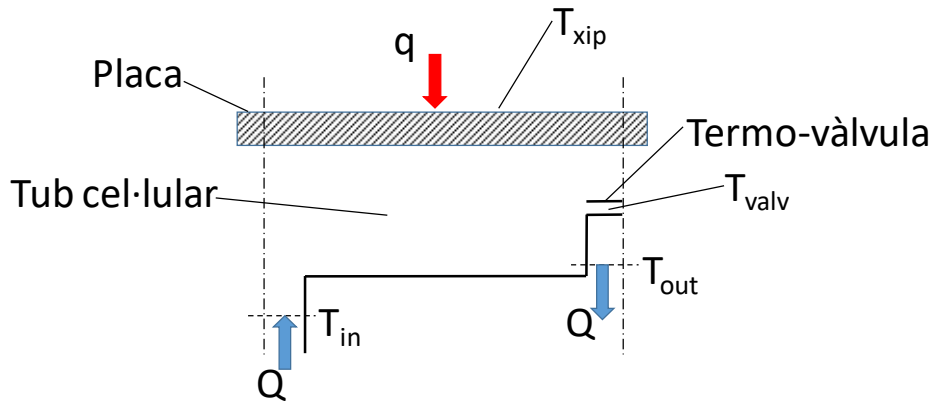


Figure 6. Microfluidic cell model

The correlation that defines the pressure losses through the valves has been obtained through the valve experimental characterization (Figure 7) carried out at LN2 (WP2).

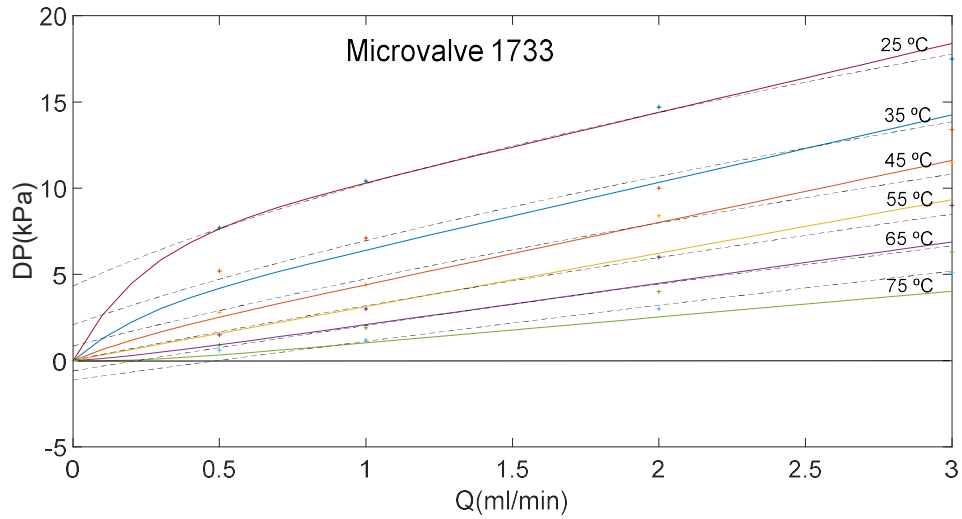


Figure 7. Comparison between the original polynomial adjustments (dotted lines, according to equation 1) and the new adjustments (color lines, equation 2). Although the polynomial adjustments are slightly better in the area where the experimental points are distributed (+), the new adjustment maintains the physical sense and produces a zero pressure drop at zero gauge.

$$DP_m = a * (1 - \exp(-z_1 * Q)) + b * Q \quad Q(\text{ml/min}), P(\text{kPa}), T(^{\circ}\text{C}) \quad (3)$$

with

$$a(T) = z_2 * \exp(-0.08 * (T - 28)) - 0.6; \quad b(T) = z_3 - ((T - 25))^2 / 1040; \quad z_1 = 4.3; \quad z_2 = 5.5; \quad z_3 = 4.0 \quad (4)$$

The resulting hydraulic model is represented in Figure 8.

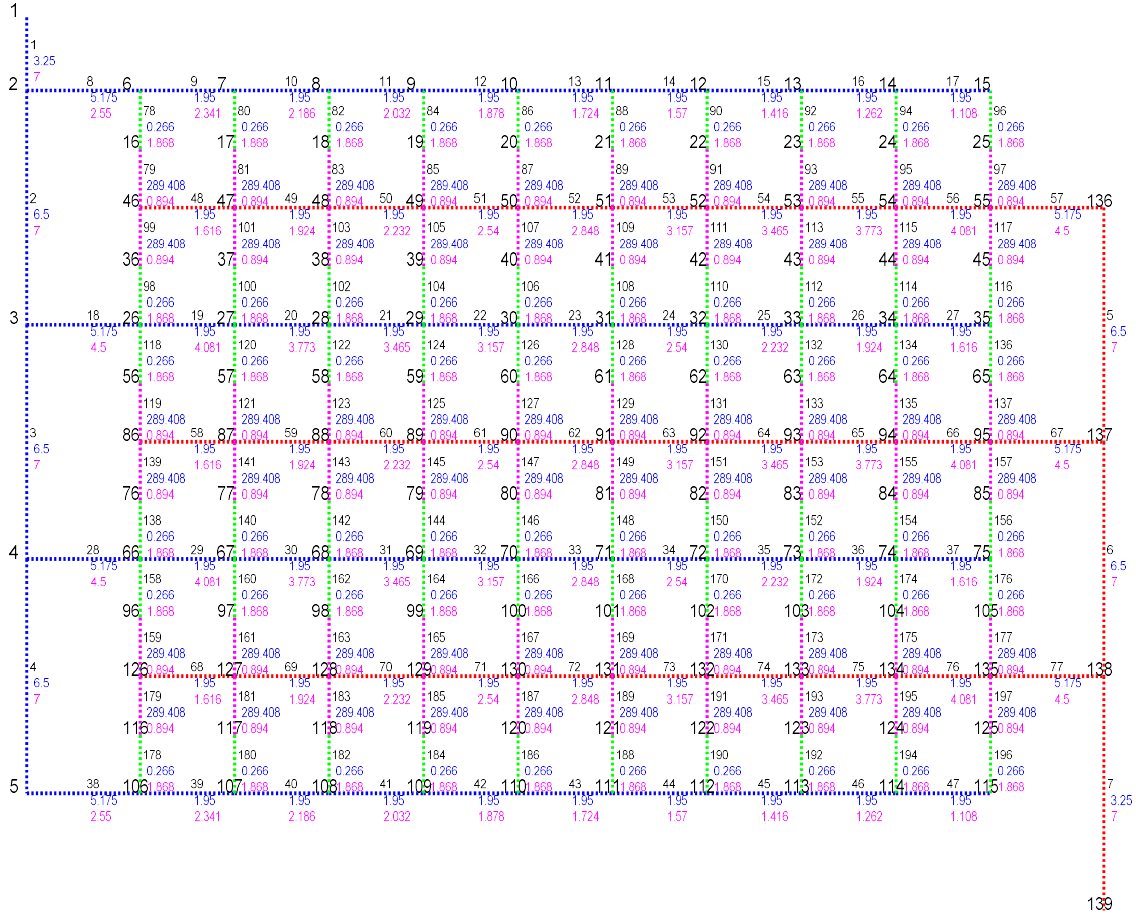


Figure 8. Hydraulic network of microchip cooling with  $m = 6$  rows and  $n = 10$  cell and side columns for coolant supply and outlets. **Legend:** Blue: feeding tubes; Red: Outlet tubes; Green: cell tubes; Magenta Thermo-valves under each cell; Black: Numbering of the nodes in the top left. Inlet node: 1, Outlet node: 139. Numbering of the tubes: in the central position: in black the tube number, below and in blue the length of the tube (mm) and below in magenta the width of the tube (mm). All non-cellular tubes have a rectangular section of height  $h = 1.4\text{mm}$ . For cellular tubes (green) and thermo-valves (magenta): in black the tube number, below and in blue the  $K_{ij}$ , and below in magenta the  $n_{ij}$  corresponding to the exponential formula of load losses  $\Delta P_{ij} = K_{ij} * Q_{ij}^{n_{ij}}$ , ( $P_{ij}[\text{Pa}]$  and  $Q_{ij}[\text{mm}^3/\text{s}]$ ). The values of  $K_{ij}$  and  $n_{ij}$  shown correspond to the opening of the valves at  $50^\circ\text{C}$ .

The coolant flow rate  $Q$  enters at temperature  $T_{in}$  into the cellular tube, heated by contact with the lower face of the plate, from which absorbs the heat flow  $q$ , and it reaches the temperature  $T_{out}$  at the outlet (location of the self-adaptive valve). The energy balance equation that governs the warming of the fluid is

$$q = \dot{m} c_p (T_{out} - T_{in}). \quad (5)$$

The heat transfer  $q$  [W] for conduction and convection between the chip board and the fluid is governed by

$$q = UA \frac{T_{out} - T_{in}}{\ln \frac{T_{chip} - T_{in}}{T_{chip} - T_{out}}} \quad (6)$$

where  $T_{xip}$  is the temperature of the chip board and  $U$  [ $W \cdot m^{-2} \cdot ^\circ C^{-1}$ ] is the global coefficient of heat transfer referred to the area of a cell plate ( $A$ ).

From equation 4, we can extract  $T_{xip}$ :

$$T_{xip} = \frac{T_{in} - T_{out} \cdot e^{\frac{UA}{q}(T_{out} - T_{in})}}{1 - e^{\frac{UA}{q}(T_{out} - T_{in})}} \quad (7)$$

This global coefficient ( $U$ ) depends on the flow rate ( $Q$ ) that circulates through the cell tube according to the ratio (cell MC6T, correlations from WP2 CFD simulations)

$$U = \frac{1}{Rth} = \frac{1}{1.09 \cdot 10^{-9} Q^{-0.620}} \quad (8)$$

In which  $Q$  is expressed in  $m^3/s$ , and is equivalent to

$$U = 2413.09 \cdot Q^{0.620} \quad (9)$$

where  $Q$  is expressed in  $mm^3/s$ . The working temperature of the valve ( $T_{valv}$ ) is given by a weighted value between the fluid output temperature ( $T_{out}$ ) and the temperature of the chip ( $T_{xip}$ )

$$T_{valv} = (1 - \xi) \cdot T_{out} + \xi \cdot T_{xip} \quad (10)$$

In the manufactured MC6T cell,  $\xi=0.25$  (correlations from WP2 CFD simulations).

#### 4.2. Boundary conditions

The simulations include three situations:

- Situation A: The hydraulic circuit has the thermo-valves blocked at an opening equal to the one they would have if they were all at a fixed temperature of  $75^\circ C$ .
- Situation B1: Thermo-valves have a variable opening depending on their temperature. The temperature of the valves is calculated from  $T_{valv} = (1 - t_{xi}) \cdot T_{out} + t_{xi} \cdot T_{xip}$ , with  $t_{xi} = 0.25$ . This value corresponds to the manufactured microfluidic cell geometry
- Situation B2: Thermo-valves have a variable opening depending on their temperature. The temperature of the valves is calculated from  $T_{valv} = (1 - t_{xi}) \cdot T_{out} + t_{xi} \cdot T_{xip}$ , with  $t_{xi} = 0.75$ .

This value corresponds to microfluidic cell geometries with the self-adaptive valves located on the same side than the surface on which the heat flux is applied

The heat load considered is defined in Figure 9.

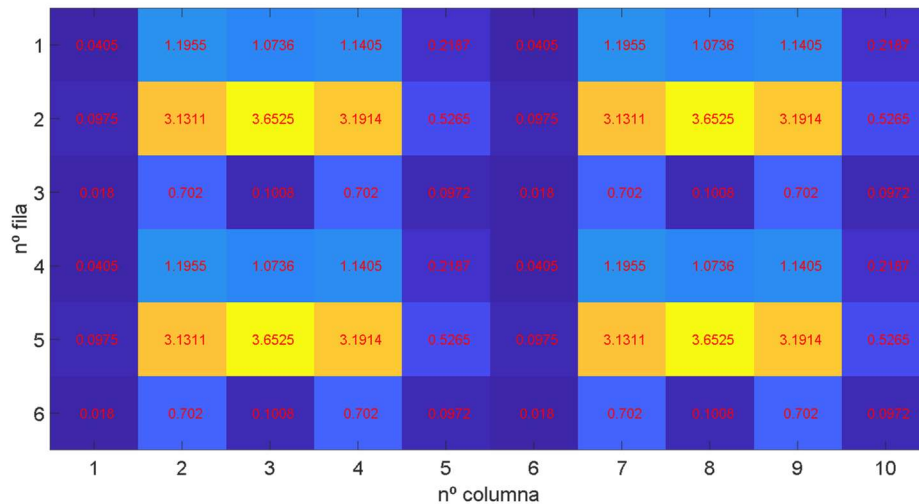


Figure 9. Heat load distribution for the set of 6 x 10 cells of the chip, (value in red on each cell,  $q$  [W]). Total thermal load:  $q = 63,55$  W.

#### 4.3. Main results

This model allows determining the impact of the self adaptive valves and the cell design on the thermo-hydraulic performance of the cooling solution, through parametric study. For example, the flow rate in a given microfluidic cell (5,8) can be determined for a given range of inlet temperatures and total pressure drop (Figure 10).

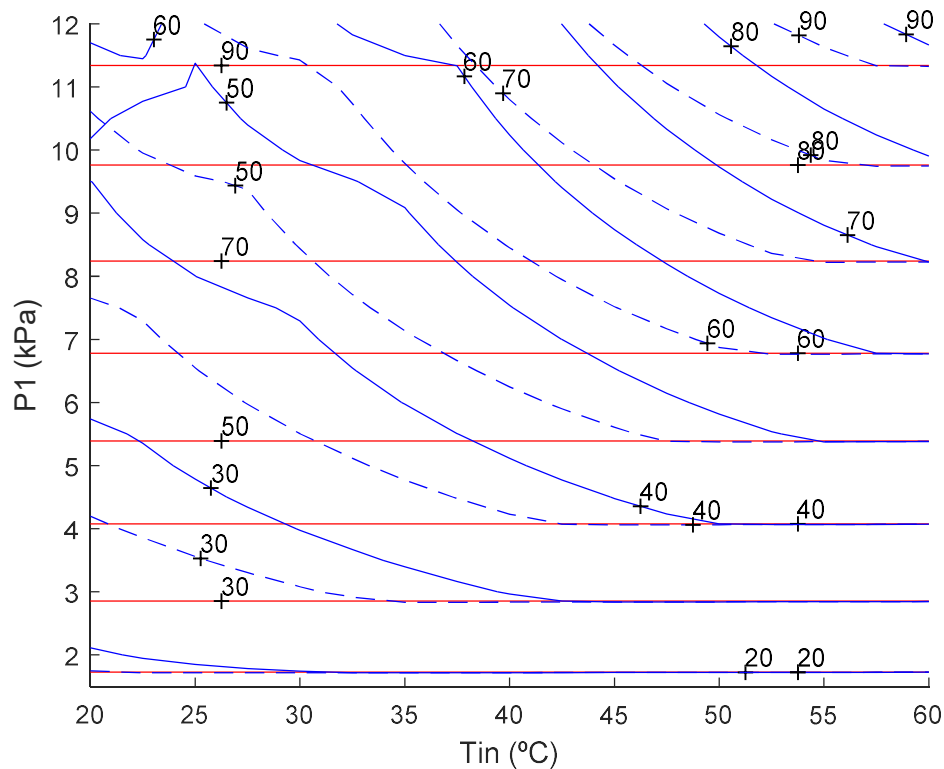


Figure 10 Flow rate  $Q1$  ( $\text{mm}^3/\text{s}$ ) of cell 1 (5.8) depending on  $T_{in}$  and  $P1$ . Red lines: thermo-valves blocked at an aperture corresponding to  $75^\circ\text{C}$  (Situation A). Continuous blue lines: Free thermo-valves and  $t_{xi} = 0.25$  (Situation B1). Discontinuous blue lines: Free thermo-valves and  $t_{xi} = 0.75$  (Situation B2).

Also, at a given total pressure drop, the model permits to assess the flow rate in a given microfluidic cell as a function of the inlet temperature (Figure 11). The flow rate self-regulation varies with the geometry of the microfluidic cell (location of the valve; Situations B1 and B2). Focusing on the fabricated samples (Situation B1, dashed lines), we can observe that the flow rate in cell 1 (5,8), which corresponds to the higher heat flux, is much lower than in Situation A (continuous line, open valves) for pressure drops of 5 and 10 kPa. The difference between both regulations reduces when the inlet temperature increases.

This characteristic implies a reduction of the pumping power (Figure 12) for the devices with flow rate regulation in each microfluidic cell (Situation B1).

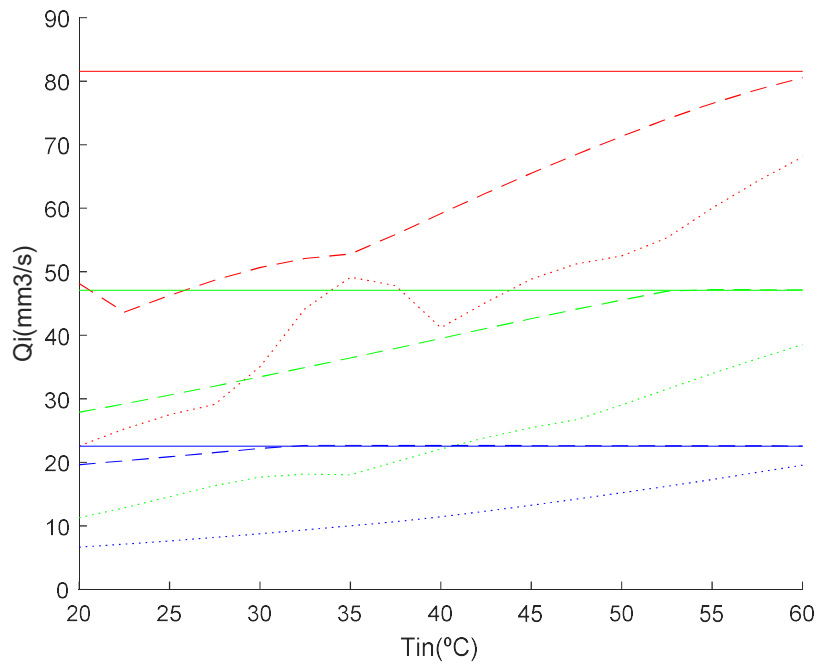


Figure 11 Effects of the inlet temperature of the coolant on the flow rates; microfluidic cell 1 (5.8); Situation A (continuous line); Situation B1 (dashed lines); situation B2 (line of points). Total pressure drop: 10 kPa (red), 5 kPa (green) and 2 kPa (blue).

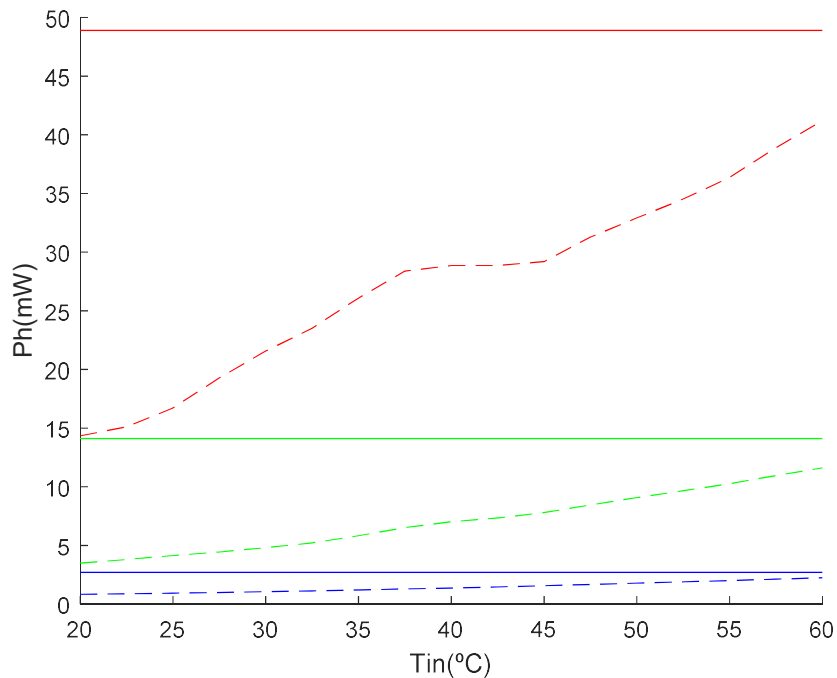


Figure 12 Total hydraulic power required  $Ph$  to circulate the cooling water according to the inlet temperature of the coolant ( $T_{in}$ ) at three different pressure drops:  $P_1 = 10$  kPa (red),  $P_1 = 5$  kPa (green) and  $P_1 = 2$  kPa (blue). Continuous lines correspond to situation A, discontinuous to situation B1.



However, the comparison is not meaningful as the chip temperature is different (Figure 13). For low inlet temperatures, the chip and valve temperatures are higher in the case of the valve regulation (Situation B1) than for the device with the valves fully opened.

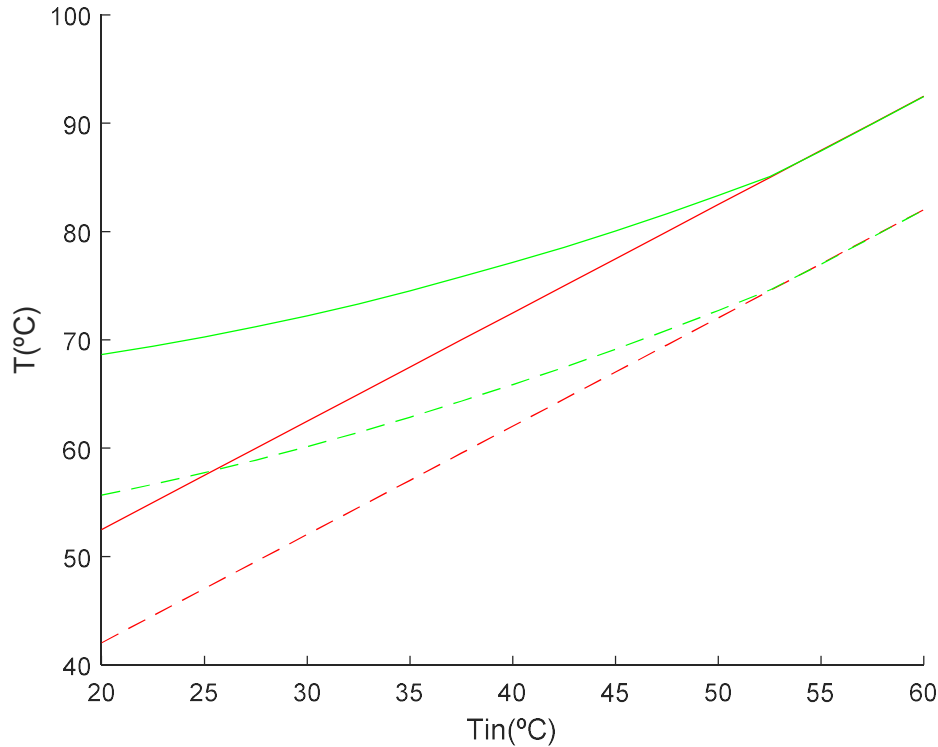


Figure 13 Chip temperature ( $T_{chip1}$ , continuous lines) and valve temperature ( $T_{valv1}$ , dashed lines) in function of the inlet temperature ( $T_{in}$ ) for the cases: A (red lines) and B1 (green lines) for a pressure drop of all the system fixed at  $P1=5$  kPa,

For this reason, new simulations have been carried out with the criteria of maintaining the maximum temperature of the chip below 85°C (Table 2).

The regulation of the flow rate distribution, through the self-adaptive valves (Situation B1), allows a Pumping power reduction of 59 and 34 % for, respectively, inlet temperatures of 20 and 50°C with respect to the device with the open valves (Situation A). This is due, mainly, to the fact that the total flow rate is reduced through the impact of the closed valves in the cells with low heat loads. The tailored flow rate distribution, which is one of the most characteristic behavior of the STREAMS cooling solution is represented through the ratio between the minimum and maximum cell flow rate. For a low inlet temperature (20°C), this ratio is up to 31. For higher inlet temperatures (50°C), even the valves of the cells with low heat loads are partially opened (the valve temperatures depends, in a big proportion, on the coolant temperature) and the ratio decreases up to 2.

Table 2 Values of the parameters that, for the indicated  $T_{in}$ , allow the operation of the system in the extreme situation in which the cell with the highest thermal load checks  $T_{xip} = 85^{\circ}\text{C}$ .

Parameter		Situation A		Situation B1	
		$T_{in} [^{\circ}\text{C}]$		$T_{in} [^{\circ}\text{C}]$	
		20	50	20	50
$P_i$	kPa	1658	4428	1922	4490
$Q_t$	$\text{mm}^3/\text{s}$	1161	2562	410	1665
$Ph$	mW	1.9	11.3	0.8	7.5
$T_{xip} \text{ m\grave{a}x}$	$^{\circ}\text{C}$	85.0	85.0	85.0	85.0
$T_{xip} \text{ min}$	$^{\circ}\text{C}$	20.3	50.2	27.0	50.3
$\text{Delt } T_{xip}$	$^{\circ}\text{C}$	64.7	34.8	57.9	34.7
$T_{valv} \text{ m\grave{a}x}$	$^{\circ}\text{C}$	70.1	74.1	70.1	74.1
$T_{valv} \text{ min}$	$^{\circ}\text{C}$	20.2	50.1	26.9	50.2
$\text{Delt } T_{valv}$	$^{\circ}\text{C}$	49.9	23.9	43.1	23.9
$Q_i \text{ m\grave{a}x}$	$\text{mm}^3/\text{s}$	19.37	42.76	19.34	42.71
$Q_i \text{ min}$	$\text{mm}^3/\text{s}$	19.33	42.68	0.62	21.08
$\text{Delt } Q_i$	$\text{mm}^3/\text{s}$	0.045	0.081	18.72	21.63
$Q_i \text{ m\grave{a}x}/Q_i \text{ min}$	-	1.002	1.001	31.19	2.02

#### 4.4. Conclusion and future works

This numerical model has shown its capacity to predict the flow rate and temperature distributions across the chip, using previous results from the experimental characterization of the self-adaptive valves and correlations from CFD simulations.

Once finished the WP2 and WP5 Proof of concepts at the very end of the project, we will focus in the next months on the experimental validation of this model. A publication is planned for the end of 2019.

The main limitation of this model is related to the necessity of external CFD simulations.

However, the program is versatile and allows implementing parametric studies with short compilation times.

## 5. IC-THERM

### 5.1. Computational model

It's not possible to simulate the entire STREAMS geometry with conventional CFD because the relatively small geometries compared to the whole device impose a thin mesh which consumes terabytes of memory and it can take several weeks to compute.

In order to make simulations of the whole system we take the program IcTherm developed by the University Polytechnic of Montreal (Transient Thermal Simulation of Liquid-Cooled 3-D Circuits by Fourmigue et al. Published at IEEE Transactions on components, packaging and manufacturing technology, VOL. 6, NO. 9, September 2016). This program should be able to simulate the entire geometry in the range of hours. This makes feasible the simulation of the entire geometry and should give us the possibility to assess different geometries.

To simulate the STREAMS geometries, the program IcTherm should be adapted because the program was designed to simulate typical 3D IC with microchannel cooling. The microchannel geometry is much simple than the one proposed by the STREAMS project having flow rate moving in the three axis dimensions in comparison to the microchannels that move only on a plane.

The program IcTherm is a program focused on the computation of heat fluxes across 3D IC cooled by microchannels technology.

The model consists in three types of heat transfer conduction, convection, and advection.

*Conduction:* In all the solid state parts of the circuit, heat transfer takes place by conduction. Conductive heat flux  $q_{cd}$  in a homogeneous medium with thermal conductivity  $k$ , can be described by Fourier's law.

$$\vec{q}_{cd} = -k \vec{\nabla} T \quad (11)$$

*Convection:* At the wall of the microchannels, the fluid velocity is rendered null by viscosity, and heat is transferred between the wall and the liquid flowing inside the microchannel. This mechanism is called forced convection, and can be described by Newton's law.

$$\vec{q}_{cv} = h(T_{wall} - T_{liquid}) \vec{n}_{wall} \quad (12)$$

The heat transfer coefficient  $h$  depends on the particular liquid considered, and on the dynamics of the flow, which are influenced by the geometry of the microchannel.

*Advection:* Advection takes place inside the microchannels, due to the energy transported by the fluid's bulk motion. Advective heat flux  $q_{ad}$  through a section  $S$  of a microchannel can be modeled using:

$$\vec{q}_{ad} = \int_S c_v T \vec{u} d\vec{s} \quad (13)$$

where  $c_v$  is the volumetric heat capacity of the fluid,  $u$  its velocity and  $T$  its temperature at the considered section.

Heat equation for liquid-cooled 3D ICs: The heat equation governs the evolution of the temperature  $T$  in time ( $t$ ) and is obtained by writing an energy balance on a volume  $V$ :

$$\int_V c_v \frac{\partial T}{\partial t} dv = \int_S \vec{q} \cdot d\vec{s} + \int_V P_{vol} dv \quad (14)$$

where  $c_v$  is the volumetric heat capacity of the material. The first term on the right is the heat exchanged through  $V$ 's surface, while the second term represents the power  $P_{vol}$  generated inside the volume  $V$ .

Solving the heat equation allows to determine the temperature everywhere in the target volume. To obtain a unique solution, the boundary conditions and the initial temperature distribution have to be specified. Solving a partial differential equation such as equation (14) is a complex task: there are no analytical methods applicable to the heterogeneous structure of 3D ICs and the various types of heat transfer involved. As a result, numerical methods are most commonly used.

Finite Difference Methods (FDMs): Finite Difference Methods use discrete approximations to replace continuous derivatives in Equation (14) by finite differences that can be more easily computed. For this purpose, the chip is discretized into small cubic cells and time is divided into small time steps  $\Delta t$ .

## 5.2. Discretization of the Heat Equation

To apply an FDM, the chip is first divided into small cubic cells, referred to as thermal cells. To handle the different materials, the circuit is divided in such a way that each thermal cell contains only one type of material, either solid or liquid.

Figure 14 shows the discretization of the chip into thermal cells and the heat flux  $q$  received by a thermal cell from the neighboring cells in the north, south, east, west, top, and bottom directions.

Using the first-order approximations of (11)–(13), the heat flux  $q_{\langle dir \rangle}$  received by the thermal cell in a particular direction can be expressed as follows:

$$q_{\langle dir \rangle} = g_{\langle dir \rangle} (T_{\langle dir \rangle} - T) \quad (15)$$

where  $g_{\langle dir \rangle}$  is the conductance between the cell and the neighboring cell in the direction  $\langle dir \rangle$ ,  $T$  is the temperature of the cell, and  $T_{\langle dir \rangle}$  is the temperature of the neighboring cell in the direction  $\langle dir \rangle$ .

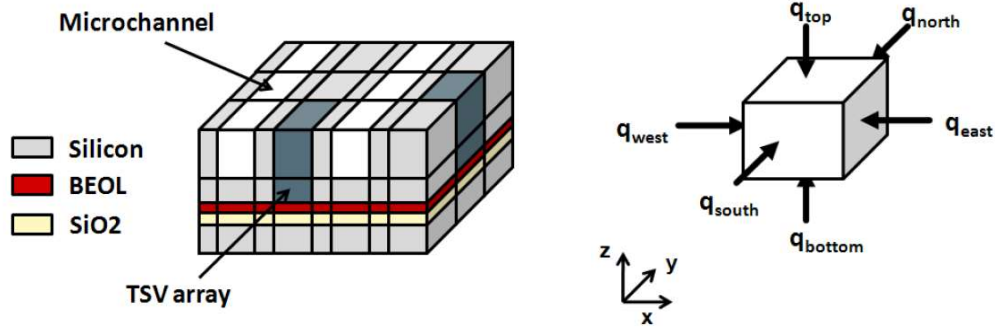


Figure 14 Mesh discretising and mesh cells orientation

For conductive and convective heat transfers, the conductance between two cells  $i, j$  can be expressed in terms of the cells' thermal resistance  $r_i, r_j$ . Note that in the case of a convective heat flux between a solid and a liquid cell, the thermal resistance of the liquid cell already includes a convective term

$$g_{i,j} = \frac{1}{r_i + r_j} \quad (16)$$

As common in other models of thermal models of liquid-cooled 3-D ICs as Relaxation, GMRES or Neural Network, we neglect contact resistance. A designer wishing to specify contact resistance can easily include it when computing the heat transfer coefficients.

For advective heat transfer inside the microchannels, the heat flux transported by the coolant as it moves from cell  $i$  to the downstream neighboring cell  $j$  can be computed as follows

$$q_{i \rightarrow j} \simeq c_v u S T_i \quad (17)$$

where  $c_v$  is the volumetric heat capacity of the coolant,  $u$  is the velocity of the coolant flow in the microchannel, and  $S$  is the section of the microchannel. Given our interest in modeling at system level and similar to all the works mentioned in Table I, we assume constant coolant velocity and neglect entrance effects for the microchannels. This simplifies the overall model without excessively impacting accuracy, since the heat-generating regions are usually relatively far from the microchannel inlets. Similarly, we do not compute pressure drops, but rather assume constant velocity for the coolant flow.

Using this formalism, the heat equation (14) is discretized and applied to each thermal cell as follows:

$$\begin{aligned} C \frac{dT}{dt} = & g_{\text{east}}(T_{\text{east}} - T) + g_{\text{west}}(T_{\text{west}} - T) \\ & + g_{\text{north}}(T_{\text{north}} - T) + g_{\text{south}}(T_{\text{south}} - T) \\ & + g_{\text{top}}(T_{\text{top}} - T) + g_{\text{bottom}}(T_{\text{bottom}} - T) \\ & + P \end{aligned} \quad (18)$$

where  $C$  is the thermal capacity of the cell,  $T$  is the temperature of the cell, and  $P$  is the power generated in the cell. This leads to a system of equations, which can be written in matrix form as follows:

$$\mathbf{C} \frac{d\mathbf{T}}{dt} = \mathbf{G}\mathbf{T} + \mathbf{P} \quad (19)$$

where  $\mathbf{C}$  is the capacitance matrix,  $\mathbf{G}$  is the conductance matrix,  $\mathbf{T}$  is the temperature vector, and  $\mathbf{P}$  is the power vector. Given that each cell is made of a single material, the heat coefficients can be easily extracted from tables of material properties or compiled for homogenized layers (BEOL for instance).

### 5.3. Solvers

To compute the steady state simulations is used an iterative method called Generalized Minimal RESidual (GMRES) to compute the transient temperature in liquid-cooled 3-D ICs. The GMRES method start using an initial approach or an initial condition. The GMRES method has two fundamental problems: 1) the cost for computing the approximate solution and 2) the method may converge very slowly or fail to converge entirely if a restart is taken. To solve this is used the method GMRES-CG, the GMRES with a preconditioner which speeds the convergence.

As GMRES-CG has to start with a guest value, if we implement GMRES-CG in the transient model we should compute a guest on each iteration it's going to be very time consuming and will slow down the simulation. For this is used the Tridiagonal Matrix Algorithm solver (TDMA).

The STREAMS system has a really small thermal inertia due to its micro-scale geometry so we focus our effort on developing the steady state simulator but we also consider to adapt the transient solver to the STREAMS geometry.

### 5.4. Usage of the initial simulator

The program from the Polytechnic of Montreal take an input file with the materials, geometry and simulation parameters required to asses the simulation.

The IcTherm reads all the information and classifies the information, creates the mesh and creates de database for all the mesh elements and the elements relation between them.

Then it's computed the transient or the steady state solver depending on which type of simulations is being computed. The results are going to be considered good if the difference between the previous iteration and the new one is lower than a tolerance or a certain number of iterations have been done. In case that any of these conditions are satisfied the solver is going to repeat the calculations taking as

initial approach the last iteration. If the condition is satisfied the temperature and flow values are saved and the simulation ends.

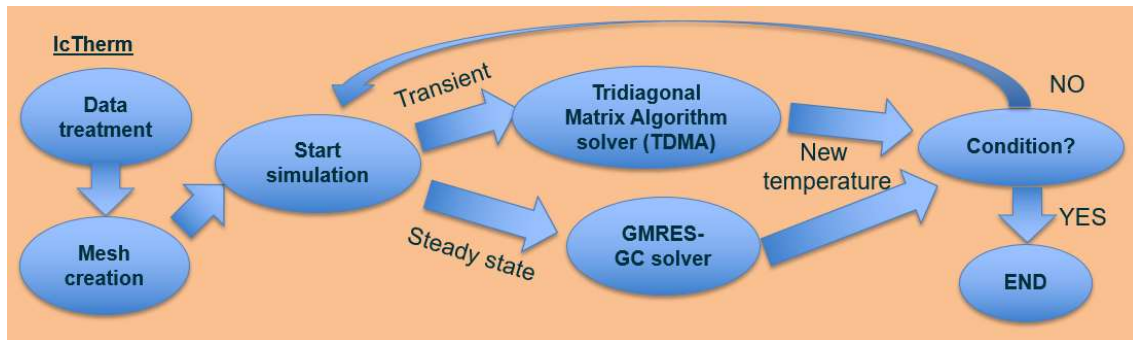


Figure 15. IcTherm initial execution scheme

### 5.5. Modifications proposal of the algorithm to adapt to the STREAMS case

In order to adapt the program to the STREAMS requirements it should be able to:

- Visualize the geometry which is going to be simulated
- Auto-adapt the flow rate in function of the temperature using the experimental data from the microvalve.
- Be able to make the relation between the distributor and the inlets/outlets of the cell. The initial program is prepared for plane microchannels and the implementation of levels of water interconnected implies an increase of the complexity.
- Add a pressure balance system in order to compute the variable flow rate of the cells.

In order to make the simulations, previously it should be done an analysis of the cell geometry with a CFD programme to determinate the pressure drop and the heat transfer coefficient in function of the flow rate. Importing this data to IcTherm is what simplifies the calculations and makes the program much faster and with less memory requirements.

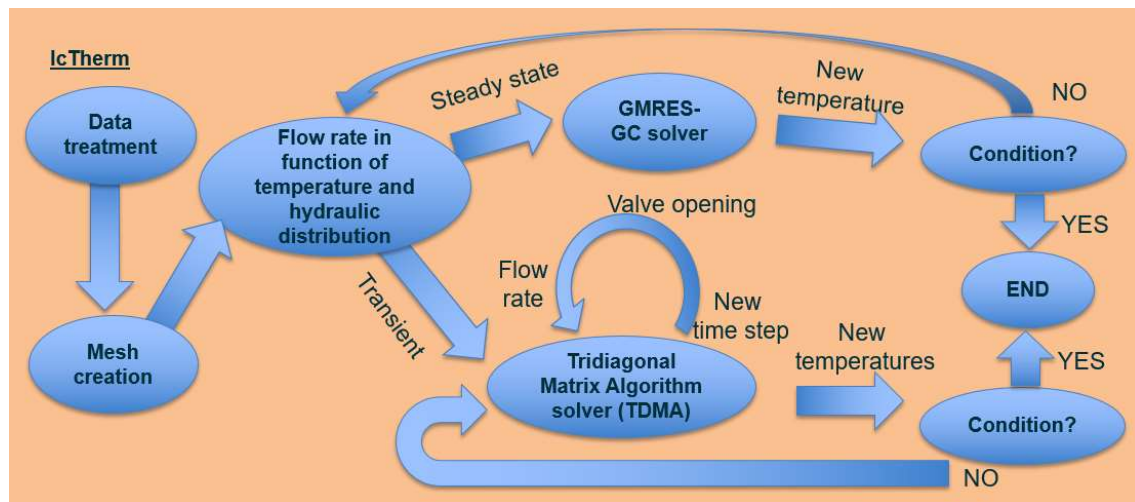


Figure 16 IcTherm proposal of modification

## 5.6. Implementation

It was created a visualizer of the imported geometry in order to visualize if the geometry was created correctly.

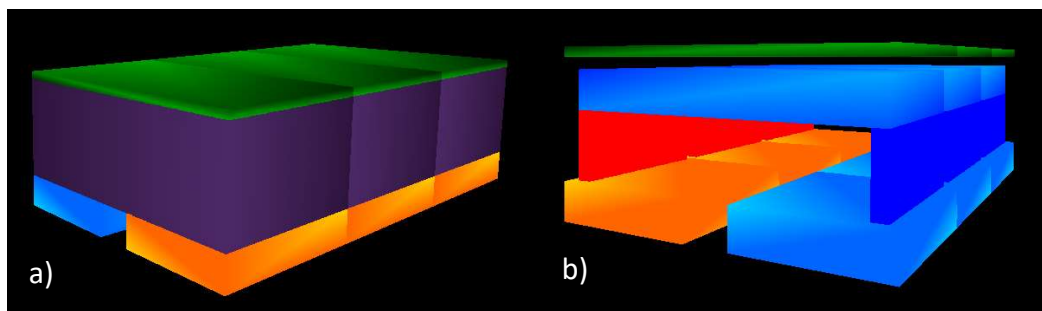


Figure 17 Visualization of a group of 3 cells a) with the silicon layer b) without the silicon layer in order to see the water path

Afterwards it was implemented the valve regulation of the flow rate and it was improved the tool which makes the relations between water path to build the fluid net in order to be able to relation paths with different directions.

## 5.7. Conclusion and future works

At this stage, the GMRES-CG computing method does not converge. We are still working on it with the objective to have a tool able to simulate this type of ICs. The potential of this tool is relevant and we plan to write a publication presenting this new tool, its interest for the electronics sector and the results of the simulations.



## 6. CONCLUSIONS AND FUTURE WORK

Through the numerical and CFD models, hydraulic and thermal models of the STREAMS devices have been achieved. However, as described in the respective chapters, they present some limitations.

IC-Therm has been identified as the right tool to achieve the Task 6.1 objectives. However, due to both its complexity and time limitations, the final version is not available at this stage.

The STREAMS team aims at implementing each of the described models and plans to publish the main results in different papers.